Comparison of Mercury Contamination in Four Indonesian Watersheds Affected by Artisanal and Small-Scale Gold Mining of Varying Scale

by Dwi Fitri Yudiantoro

Submission date: 26-Aug-2019 11:35PM (UTC+0700)
Submission ID: 1163671680
File name: 5._September_2019-Comparison_of_mercury.pdf (16.23M)
Word count: 9154
Character count: 47914

Water Air Soil Pollut (2019) 230:214
https://doi.org/10.1007/s11270-019-4271-1

Comparison of Mercury Contamination in Four Indonesian Watersheds Affected by Artisanal and Small-Scale Gold Mining of Varying Scale

Natalie M. Barkdull · Gregory T. Carling · Kevin Rey · Dwi Fitri Yudiantoro

Received: 13 May 2019 / Accepted: 14 August 2019

Abstract Artisanal and small-scale gold mining (ASGM) accounts for almost half of anthropogenic mercury (Hg) emissions worldwide and causes widespread water pollution. In Indonesia, several studies have identified harmful levels of Hg in areas affected by ASGM. While most of these studies focus on mining areas with thousands of miners, water contamination in smaller ASGM areas is less understood. We evaluated Hg contamination in four ASGM areas in Central Java of varying scale (from 30 to 3000 amalgamator barrels at each area), including Jatiroto, Kebonsari, Gumelar, and Kulon Progo. At each location, we collected water samples along river transects upstream and downstream of ASGM areas during the dry season (June–July 2017). Total Hg (THg) concentrations in stream water increased by orders of magnitude from upstream to downstream of ASGM activities at Jatiroto (1.35–4730 ng/L), with smaller observed increases at the other locations. Dissolved THg concentrations exceeded USEPA criteria for aquatic life (12 ng/L) at two of the four ASGM areas. THg concentrations in tailings exceeded 150,000 ng/L. Notably, THg concentrations in stream water were not directly related to the scale of mining, with Jatiroto having the highest concentrations as second smallest mining areas of the four in this study. Downstream of the mining areas, the fraction of dissolved methyl Hg to dissolved THg reached 20%, indicating that active Hg methylation occurs in the watersheds. Further study is needed to investigate Hg transport in the wet season when rainfall and high stream discharge may mobilize contaminated sediment near mining areas.

Keywords Trace elements · Total mercury · Methyl mercury · Artisanal and small-scale gold mining · ASGM · Indonesia

Electronic supplementary material The online version of this article (https://doi.org/10.1007/s11270-019-4271-1) contains supplementary material, which is available to authorized users.

N. M. Barkdull · G. T. Carling (✉) · K. Rey
Department of Geological Sciences, S389 Eyring Science Center, Brigham Young University, Provo, UT 84602, USA
e-mail: greg.carling@byu.edu

D. F. Yudiantoro
Geology Department, Jl. SWK 104 (Lingkar Utara) Condongcatur, Universitas Pembangunan Nasional Veteran Yogyakarta, Yogyakarta 55283, Indonesia

1 Introduction

Mercury (Hg) is a global pollutant that threatens human and environmental health. The largest source of anthropogenic Hg emissions is the artisanal and small-scale gold mining (ASGM) industry (AMAP/UNEP 2013). Millions of small-scale miners in over 70 countries use inexpensive technology to search for, process, and extract gold (Telmer and Veiga 2009). In Indonesia, the world's third-largest Hg emitter, over a million people in hundreds of mining areas use Hg to extract and concentrate gold in a process called whole-ore amalgamation (Ismawati et al. 2013; AMAP/UNEP 2013). Over 75% of the Hg used in whole-ore amalgamation is discharged to the environment, contaminating fish, crops, and ASGM workers themselves (Bose-O'Reilly et al. 2010; Krisnayanti et al. 2012;

Published online: 22 August 2019

Limbong et al. 2003). Indonesians living and working in ASGM areas show symptoms of Hg intoxication and elevated Hg concentrations in blood, hair, and urine compare to nonmining areas (Bose-O'Reilly et al. 2010). ASGM also contaminates rice and fish cultivated near or downstream of gold processing activities (Castilhos et al. 2006). Although Indonesia has prohibited the use of Hg for ASGM, widespread Hg use continues, driven by domestic cinnabar production and the high price of gold (Spiegel et al. 2018). While many studies have examined Hg pollution in large Indonesian ASGM areas with hundreds of miners and amalgamators, relatively little attention has been given to smaller ASGM areas (Iqbal and Inoue 2011; Ismawati et al. 2013).

Mercury from ASGM areas can enter the environment through several pathways. Elemental Hg used in ASGM converts to Hg^0 vapor or is oxidized to Hg^{2+}, the prevalent form of Hg in aquatic environments (Swartzendruber and Jaffe 2012). Hg^0 vapor released during amalgam smelting enters the atmosphere and may be redeposited in local rain or undergo long-range atmospheric transport (Obrist et al. 2018). Hg^{2+} is transported from mining areas through erosion of contaminated soil or dissolved in stream water. Most Hg transport in streams occurs during episodic events like storms and seasonal runoff, when Hg is mobilized from sediment and soil water or resuspended from the stream bed (Bishop et al. 1995; Whyte and Kirchner 2000; Schuster et al. 2008; Hurley et al. 1998). A small fraction of Hg^{2+} is converted to methyl Hg (MeHg) by sulfate- (SO_4^{2-}) or iron-reducing bacteria in anoxic environments like wetlands, rice fields, or reservoirs (Shanley and Bishop 2012). MeHg is more toxic than inorganic Hg because it bioaccumulates in the aquatic and terrestrial food web (Rothenberg et al. 2014; Scheuhammer 1987; NRC 2000; Clarkson 1997). Methylation is prevalent in tropical areas like Indonesia because waters are typically anoxic, rich in dissolved organic carbon (DOC), and alternate between wet and dry conditions (Rothenberg et al. 2017; Rothenberg et al. 2014; Shanley and Bishop 2012).

Specific trace elements found in ASGM tailings, such as Al, Cd, Cr, Cu, Hg, Ni, Pb, Se, and Zn, may negatively impact aquatic life. These trace metals are transported from ASGM areas downstream in many forms such as dissolved ions, metal complexes with dissolved organic matter, or metals adsorbed on the surface of colloidal particles like clay depending on bulk water chemistry (Gaillardet et al. 2003; Carling et al. 2013; Yasuda et al. 2011). Water chemistry, including pH, temperature, and major ion chemistry, determines the speciation of trace metals. Metals transported as particulates or organic complexes are less bioavailable than dissolved ions and may not travel as far downstream depending on the suspended sediment load of the river (Luoma 1983). Cation-forming trace metals (Cr, Pb, Cu, Cd, Zn, Ni) adsorb to particles at high pH while anion forming elements (SeO_4^{2-}, CrO_4^{2-}, $VO4^{2-}$, AsO_4^{3-}) adsorb at low pH (Sigg et al. 2001). Weathering of tropical soils produces clay particles that efficiently adsorb and transport trace metals (Telmer and Veiga 2009). Many trace metals such as Hg are also transported downstream attached to DOC (Shanley and Bishop 2012). Thus, it is important to understand total water chemistry to investigate trace metal transport from ASGM areas.

We examined Hg contamination in river water and mine tailings from four rural communities affected by ASGM activities on the densely populated (> 141 million people) island of Java, Indonesia (Fig. 1). The goals of our study were to (1) quantify particulate THg, dissolved THg, and dissolved MeHg concentrations in river water upstream and downstream of ASGM affected areas; (2) compare THg concentrations between four different mining areas in relation to the scale of mining; and (3) evaluate the effect of water chemistry on THg concentrations and transport. While other studies have focused on the largest ASGM areas near Jakarta, this study is unique because it compares water chemistry across four small ASGM areas in rural Java.

2 Methods

2.1 Previous ASGM Studies in Indonesia

Previous studies of ASGM in Indonesia examined the effects of Hg pollution on the health of ASGM workers and local communities in large mining areas with thousands of gold amalgamators (Iqbal and Inoue 2011; Ismawati et al. 2013). For example, almost all the residents of Palu City, South Sulawesi, were exposed to toxic levels of atmospheric Hg^0 from gold smelting in ASGM areas (Nakazawa et al. 2016). Symptoms of Hg intoxication (ataxia, tremors, central nervous system damage) were also observed across large ASGM communities in Kalimantan and Sulawesi at rates between 23.5 and 62.3% (Bose-O'Reilly et al. 2010). However, Hg-contaminated water and sediment also affect communities downstream of ASGM particularly through Hg bioaccumulation in fish and rice (Rothenberg et al. 2014; Sherman et al. 2015). For example, over 45% of fish collected downstream of

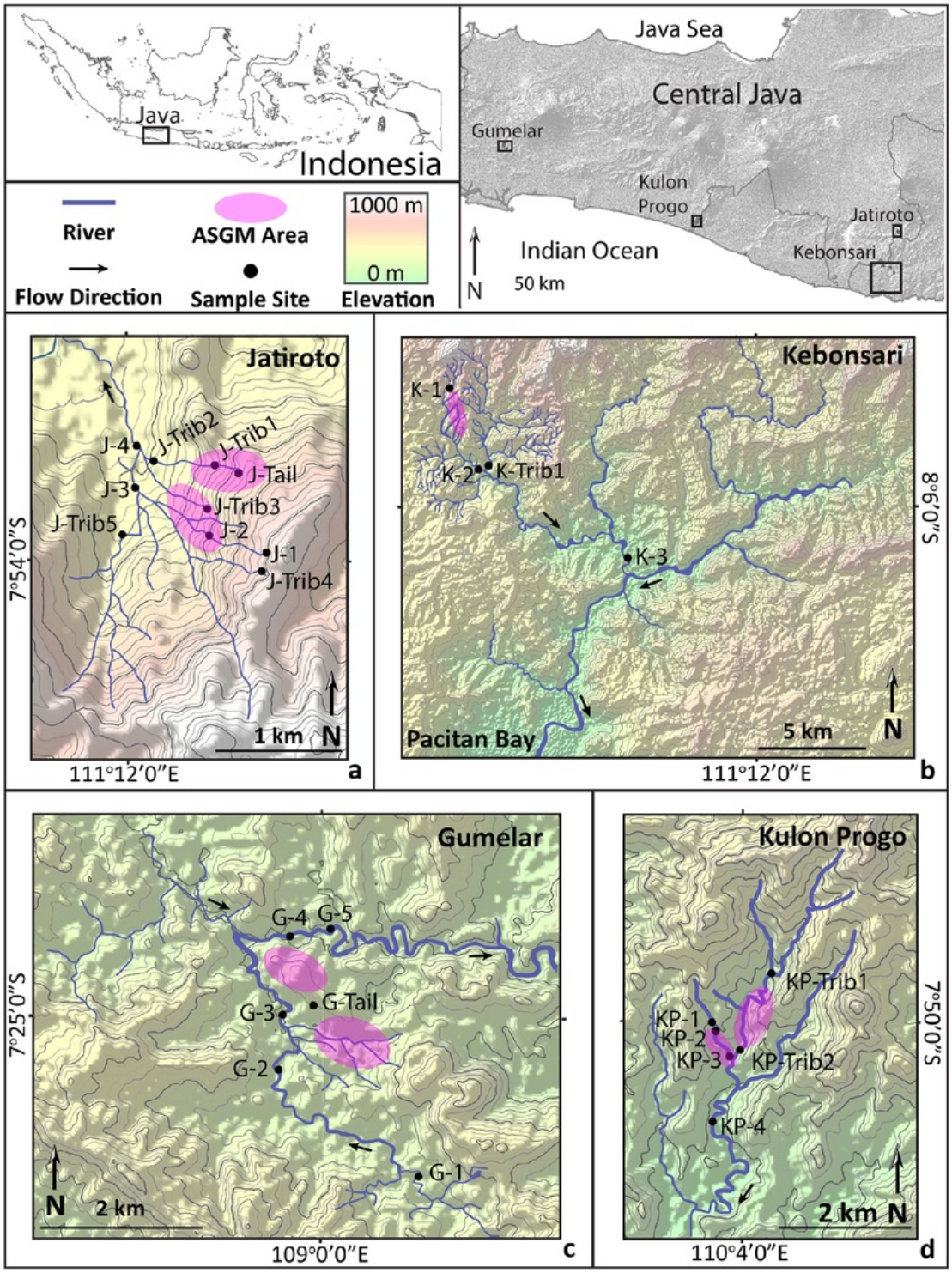

Fig. 1 Water sampling locations at four ASGM areas in Java, Indonesia. **a** Jatiroto, Wonogiri Regency. **b** Kebonsari, Pacitan Regency. **c** Gumelar, Banyumas Regency. **d** Kulon Progo, Daerah Istimewa Yogyakarta Regency. Elevation in meters above sea level

ASGM areas in Sulawesi contained Hg levels above the World Health Organization (WHO) guideline for human consumption at 0.5 μg/g (Castilhos et al. 2006). Hg concentrations in rice grains cultivated downstream of an ASGM area in Lombok also reached five times the Chinese permissible level for Hg in food crops (Krisnayanti et al. 2012). While many studies have examined Hg concentrations in sediment and tailings from ASGM activities (Limbong et al. 2003; Elvince et al. 2008; Harijoko et al. 2010; Beavis and McWilliam 2018), we focused on dissolved (< 0.45 μm) and particulate (> 0.45 μm) Hg concentrations in rivers as an indicator of Hg transport downstream. To our knowledge, no studies have quantified aquatic dissolved THg, particulate THg, and dissolved MeHg concentrations downstream of ASGM areas in Indonesia, particularly smaller ASGM areas.

2.2 Site Description

To investigate aquatic Hg transport and potential for Hg methylation related to ASGM, we collected water samples at four areas on the island of Java, Indonesia (Fig. 1). Water sampling was conducted to characterize stream chemistry upstream, within, and below gold processing zones during low flow conditions in the dry season (June–July). The four areas were: Jatiroto, Wonogiri Regency; Kebonsari, Pacitan Regency; Kulon Progo, Daerah Istimewa Yogyakarta Regency; and Gumelar, Banyumas Regency (Fig. 1). The bedrock geology of the sampling sites consists of Oligo-Miocene volcanic rocks, reworked volcaniclastic deposits, and carbonate rocks (Smyth et al. 2008). The four watersheds are located on the south side of the island of Java, with similar climate and topography. Kebonsari is the largest watershed followed by Gumelar, Kulon Progo, and Jatiroto. The ASGM-impacted area at the headwaters of each watershed was approximately 16 km^2 in Kebonsari, 15 km^2 in Gumelar, 5 km^2 in Kulon Progo, and 2 km^2 in Jatiroto. The scale of mining operations varied in each community from 30 operating amalgamator barrels at Kulon Progo to 3000 barrels at Gumelar (Table 1). Since water quality in ASGM areas fluctuates depending on sporadic releases of contaminants and changes in seasonal flow, our sampling represents a "snapshot" during the dry season.

Whole-ore amalgamation is the primary Hg extraction method used in each of the four small ASGM areas (Fig. 2). Briefly, gold-bearing ore is removed from hand-dug shafts and pits reaching 50 m deep (Fig. 2a, b). Ore is crushed on site and bagged for transport to processing locations in residential backyards (Fig. 2c). Hg-gold amalgamation typically takes place in residential areas because many miners split time between cultivating rice fields and processing ore in homemade amalgamator barrels called *tromol* mills. At the processing site, the gold bearing ore is crushed using heavy metal rods (*gelendong*) in a tumbler (*tromol*) and combined with elemental Hg (Fig. 2f). Workers use 1 kg Hg per amalgamator barrel of sediment and tumble 4–8 h to form a Hg-gold amalgam (Fig. 2g). The resulting amalgam is burned, often indoors, exposing residents to harmful Hg vapor levels (Fig. 2i) (Bose-O'Reilly et al. 2010). Hg-laden tailings pile up in backyards and may contaminate downstream areas (Fig. 2d, e).

2.3 Water Sample Collection

Water samples were collected upstream, within, and downstream of ASGM areas during June and July 2017 (Fig. 1).

Table 1 Estimated annual Hg use compared to measured Hg concentrations in each ASGM area

Area	Scale of mining (# amalgamator barrels)	Total Hg use (t/year)		THg concentrations (ng/L)			THg
		low	high	Dissolved THg (< 0.45 μm)	Particulate THg (> 0.45 μm)	Unfiltered THg	(highest to lowest)
Kulon Progo	30	4.93	7.67	0.87–9.90	0.42–101	1.48–106	3
Jatiroto	100	16.4	25.6	2.51–57.0	6.74–4673	9.84–4730	1
Kebonsari	300	49.3	76.7	0.81–2.58	0.54–7.31	1.35–9.89	4
Gumelar	3000	493	767	2.46–27.0	12.3–228	15.9–255	2

Fig. 2 ASGM activities across study area in Java, Indonesia. **a** Open pit mining in hilly areas of Jatiroto. **b** Wooden cart on bamboo runners used to remove gold-bearing ore from mine shaft. **c** Workers bag gold-bearing ore near open pit mines for transport to ore-processing area. **d** Bags of fresh gold ore are crushed in the gelendong with metal rods. Water and 1 kg Hg are added and tumbled between 2 and 4 h to form a Hg/gold amalgam. The tumbling barrel is washed out and the sediment panned for gold. Tailings are dumped in a pile nearby or allowed to wash downhill. **e** Local miner in Kebonsari displays gelendong setup behind his home. **f** Empty Hg bottles used by miners in Kebonsari. **g** Miner rinses out amalgamator barrels in Gumelar. **h** Mine worker in Gumelar rinses sediment to pan for gold amalgam. **i** Hg retort used to burn Hg/gold amalgam

At Jatiroto, we collected four samples from the main stream (J-1 through J-4), five samples from tributaries (J-Trib1 through J-Trib5), and one sample from amalgamator waste tailings (J-Tail). At Kebonsari, we collected three samples from the main stream (K-1 through K-3) and one sample from a tributary (K-Trib1). At Gumelar, we collected five samples from the main stream (G-1 through G-5) and one sample from amalgamator waste tailings (G-Tail). At Kulon Progo, we collected four samples from the main stream (KP-1 through KP-4) and two samples from a tributary (KP-Trib1 and KP-Trib2).

Samples were filtered directly from the stream using a peristaltic pump with precleaned Teflon tubing and a 0.45 μm high capacity disposable Geotech cartridge filter. Water was collected from the main current of the stream to obtain a representative sample. Temperature (°C), specific conductance (μS/cm), dissolved oxygen (mg/L), pH, and ORP (mV) were measured on site with a YSI Quattro

Professional Series multiparameter probe. Turbidity was measured using a MicroTPW Turbidimeter Field Portable Probe and bicarbonate concentrations were measured using low-range HACH Alkalinity Test Kits.

Water samples were collected for Hg, bulk chemistry, δD, and $\delta^{18}O$. Filtered (< 0.45 μm) and unfiltered water samples were collected for total Hg (THg) and MeHg. THg and MeHg samples were collected in double-bagged Milli-Q rinsed 250 mL FLPE bottles and acidified to 1% *v*/*v* with trace metal grade HCl. Filtered water samples were collected for DOC and total N (TN), major cations (Ca, K, Mg, Na), trace elements (Ag, Al, As, Ba, Be, Cd, Co, Cr, Cu, Fe, Li, Mn, Mo, Ni, Pb, Sb, Se, Sr, Ti, Tl, U, V, Zn), and major anions (F^-, Cl^-, NO_3^-, SO_4^{2-}). Trace element and major cation samples were collected in acid-leached, single-bagged 60 mL LDPE bottles and were acidified to 2.4% *v*/*v* with trace metal grade HNO_3. DOC samples were collected in 60 mL ashed amber bottles capped with ashed aluminum foil and preserved by acidifying to pH < 2 with concentrated HCl. Unfiltered samples were collected for δD and $\delta^{18}O$ isotopes in water. Field blanks were collected to test for contamination during the sampling process including collection, storage, analysis, and handling of samples. Field blank collection followed the same protocols as stream sampling.

2.4 Laboratory Analysis

Filtered and unfiltered THg samples were prepared according to US Environmental Protection Agency (USEPA) Method 1631e and analyzed using a Brooks Rand Merx-T cold vapor atomic fluorescence spectrometer after BrCl oxidation (CVAFS) (USEPA 2002). As a quality control, matrix spikes were made at least every 10 samples with recoveries between 83 and 100%. Filtered MeHg samples were prepared by direct ethylation (Mansfield and Black 2015) and analyzed on the Brooks Rand Merx-M system. As a quality control, a 1 ng/L matrix spike was made for each sample with recoveries between 88 and 132%. Method blanks were analyzed at the beginning of each run to calculate the detection limit (DL), which was typically below 0.2 ng/L for THg and 0.02 ng/L for MeHg. The "particulate" THg fraction was calculated as the difference between unfiltered and filtered concentrations. The filtered fraction was considered "dissolved," although Hg is likely associated with colloidal particles smaller than 0.45 μm (Babiarz et al. 2001).

Filtered water samples were analyzed for major cations and trace elements using a Thermo Scientific Inductively Coupled Plasma Optical Emission Spectrometer (ICP-OES) iCAP 7400 Duo Series. The instrument was calibrated with inorganic ventures IV-ICPMS-71A and 71B aqueous solutions for trace elements (Al, As, B, Ba, Ca, Fe, K, Li, Mg, Mn, Mo, Na, P, Pb, Sb, Se, Si, Sr, Tl, V, Zn) and the IV-Stock-50 for major cations (Ca, Fe, K, Mg, Na). A standard of a known concentration of IV-ICPMS-71A and 71B was analyzed with every 10 samples to check for instrument drift. An independent standard (High Purity Solutions) was analyzed with a subset of samples to verify accuracy of measurements. Total anions (F, Cl, Br, NO_3, HPO_4, SO_4) were analyzed by ion chromatography (IC) with a Dionex ICS-90 Ion Chromatography System. Charge balances were calculated for each sample to ensure accuracy of bicarbonate, anion, and cation concentrations. Each sample had a charge balance error within ± 5%.

Oxygen ($\delta^{18}O$) and hydrogen (δD) stable isotopes in water were analyzed using a Los Gatos Research LWIA-24d cavity ringdown spectrometer. The instrument was calibrated with each set of samples using standards traceable to Vienna Standard Mean Ocean Water (VSMOW) with an analytical precision of ± 0.4% for $\delta^{18}O$ and ± 1% for δD. DOC and TN were analyzed using a Shimadzu TOC-5000A. Raw water chemistry data are provided in the Supplementary material (Table S1).

2.5 Water Classification and Geochemical Modeling

Major ion and trace element chemistry at each site was evaluated and categorized using The Geochemist's Workbench (GWB) software (Bethke et al. 2018). A Piper diagram was created in GWB to classify water type for each sample. Aqueous speciation and saturation indices (SIs) were calculated in the SPEC8 feature of Geochemist's workbench using the LLNL thermodynamic database. Positive SI values, calculated as log (IAP/K_{SP}), indicate oversaturation and thermodynamic potential for mineral precipitation. GWB uses ion-association and modified Debye-Huckel expressions to account for the nonideality of aqueous solutions. Water temperature, pH, and dissolved concentrations of major ions and trace elements measured at each site were used in the simulations.

Nonmetric multidimensional scaling (NMS) was used to compare major and trace element chemistry between river samples from each site. NMS is an ordination technique that simplifies data dimensionality to explain similarities and differences between

groups of samples. NMS is like principal component analysis (PCA) but does not assume linear relationships between variables and is suited for a wider variety of datasets (McCune and Mefford 1999). We used NMS to characterize water sample chemistry, including pH, specific conductance (cond), DOC, TN, major ions (Na^+, K^+, Mg^{2+}, Ca^{2+}, F^-, Cl^-, HCO_3^-, SO_4^{2-}), 13 trace elements (Al, As, Ba, Cu, Fe, Mn, Mo, P, Pb, Sr, Ti, V, Zn), and three Hg fractions (unfiltered THg, dissolved THg, and dissolved MeHg). Elements that were below DL for over half of the samples were not used in NMS. For other elements, values below DL were set as one half the DL. Raw data used in the NMS ordination are provided in the Supplementary material (Table S2).

PC-ORD (McCune and Mefford 1999) was used for the NMS ordination. Data were log generalized prior to performing the NMS analysis using the equation $b = \log(x + x_{min}) - \log(x_{min})$ where x_{min} is the minimum concentration of each element. Euclidean distance was used to assign the samples in ordination space. The analyses were run 250 times and compare to randomized data in a Monte Carlo test run with 250 iterations. The final model had a stable 2D solution with a low stress value, which is a measure of the goodness of fit for the model.

3 Results

3.1 Water Chemistry Comparison Across Sites

The Piper diagram showed similar water types in each watershed based on dominant cation and anion species (Fig. 3). Waters from each sample site were dominated by carbonate and alkaline earth metals (Ca^{2+}, Mg^{2+}). Ca^{2+} was the dominant cation in Kulon Progo and Gumelar. The dominant cation in Kebonsari and Jatiroto was split between Mg^{2+}, Ca^{2+}, and to a lesser degree, Na^+/K^+. Waters from each site were slightly alkaline with an average pH between 7.4 and 8.2 although samples K-1 and J-7 were circumneutral (pH 6.6 and 7.1, respectively). The pH of amalgamator waste tailings at Jatiroto and Gumelar (pH < 7) was lower than water from the surrounding areas (pH > 7).

The tailings sample from Jatiroto was distinct from the tailings sample from Gumelar (Fig. 3). Tailings from Jatiroto were Mg^{2+}/Ca^{2+}–HCO_3 type like nearby river water. In contrast, tailings from Gumelar were Mg^{2+}/Ca^{2+}–SO_4^{2-} type while nearby streams were by Ca^{2+}–HCO_3^- type. Gumelar tailings contained much higher solute concentrations, including 200 times more SO_4^{2-}, relative to Jatiroto tailings.

The tailings samples had high concentrations of specific trace elements. At Jatiroto, B, Mo, and Se were higher in tailings relative to river samples. At Gumelar, B, Co, Ba, Fe, Mn, Ni, Sb, Se, Sr, Ti, Tl, and Zn concentrations were higher in tailings relative to river samples. Al, Cu, Mo, Pb, Si, and V concentrations were higher in Jatiroto tailings relative to Gumelar tailings, while concentrations of As, B, Ba, Cd, Co, Cr, Fe, Mn, Ni, Sb, Se, Sr, Ti, Tl, and Zn were higher in Gumelar tailings relative to Jatiroto tailings. For a complete list of water chemistry at each sample, see Supplementary material (Table S1).

Besides THg, most trace element and major ion concentrations did not increase dramatically from upstream to downstream of ASGM processing areas (Supplementary material, Table S1). Dissolved trace metal concentrations did not exceed USEPA guidelines for drinking water; however, samples from Jatiroto and Kulon Progo exceeded USEPA continuous criterion Pb limits for aquatic life (Supplementary material, Table S3).

Isotope values (δD and $\delta^{18}O$) for all samples plotted near the local meteoric water line for Java, Indonesia (IAEA/WMO 2019) (Supplementary material, Fig. S1). δD and $\delta^{18}O$ varied most in Jatiroto, where upstream samples (J-1 and J-2) were more depleted relative to downstream samples (J-3 and J-4). Tailing samples were also isotopically depleted relative to nearby streams. TN concentrations ranged from 0.46 to 3.35 mg/L while DOC concentrations ranged from 1.37 to 9.65 mg/L. There were no observable trends upstream of downstream of mining operations for either DOC or TN; however, the highest DOC concentrations were measured in samples near agricultural discharge. The ratio of DOC to TN varied from 0.6 to 8.7 with an average value of 3.3. Results for TN, DOC, δD, and $\delta^{18}O$ are provided in Supplementary material (Table S1).

3.2 NMS Ordination

The NMS ordination identified differences between major ion and trace element concentrations between each site (Fig. 4). The two-axis model explained almost 95% of total variance in the dataset. The best fit NMS model had a stress value of 8.61, where stress values < 10 are considered valid for interpretations (McCune and

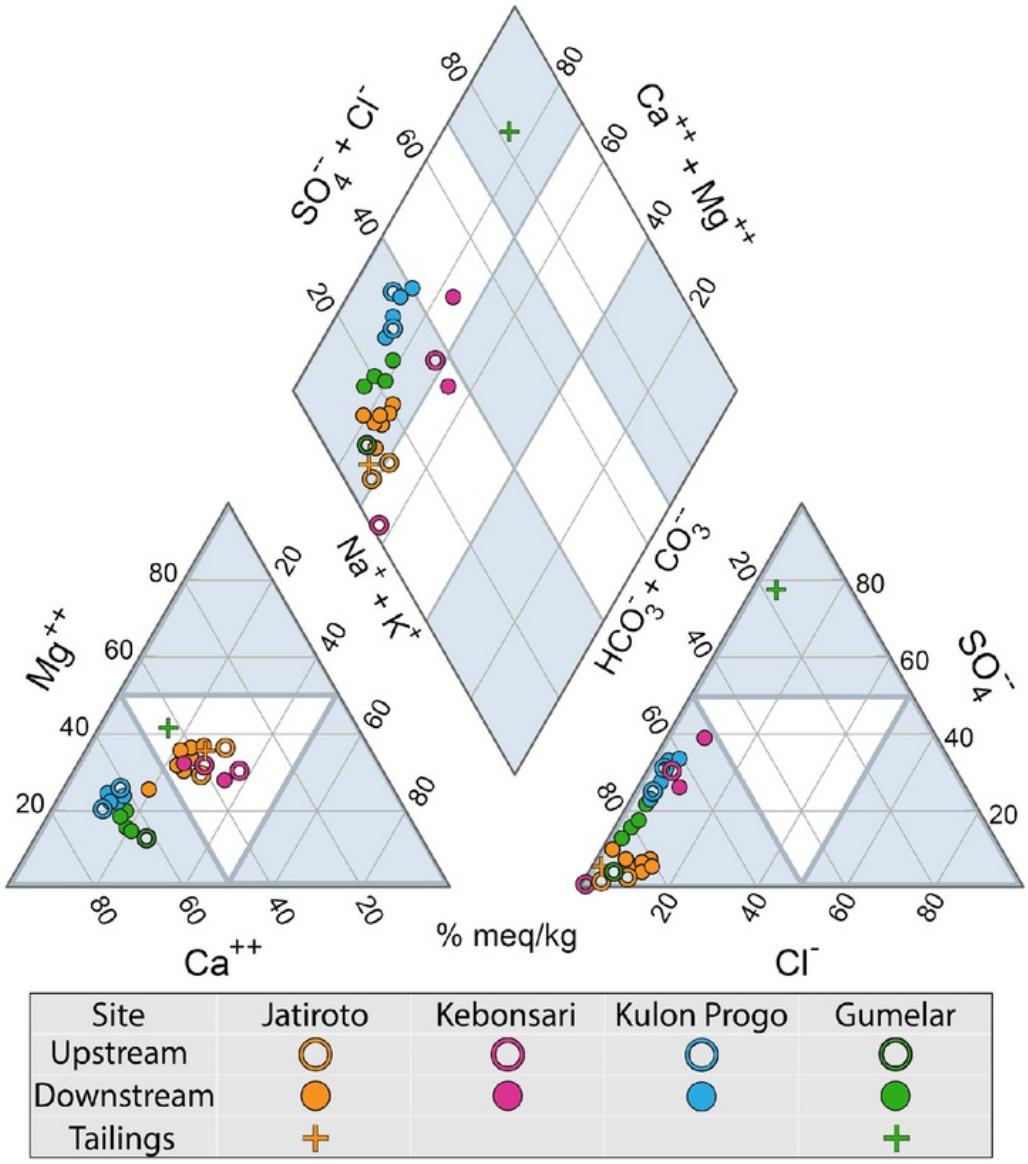

Fig. 3 Piper diagram showing the relative contributions of major ions to ionic charge in each sample. The bottom left ternary diagram shows major cations and bottom right diagram shows major anions controlling water chemistry. Both ternary diagrams are projected onto a diamond in the center diagram to determine the hydrochemical facies of each sample. Blue and white shaded areas outline distinct hydrochemical facies

Mefford 1999). In the ordination, samples from each site are clustered based on similar chemistry. Axis 1, which explained 72% of the variance in the dataset, was structured by samples with elevated THg concentrations to the right, and samples with higher concentrations of several trace elements and variables, including Fe, Al, Mn, Ba, Ti, Zn, Cu, SO_4^{2}, TN, pH, and DOC, to the left. Axis 2, which explained 22.9% of the variance in the dataset, was controlled by samples with elevated Fe, Al, and THg concentrations at the top, and samples with increasing concentrations of Ba, Ti, Sr, major ions (Na^+, K^+, Mg^{2+}, Ca^{2+}, Cl^-, HCO_3^-, and SO_4^{2-}), and specific conductance at the bottom.

Water samples from Kebonsari and Jatiroto were chemically distinct from those at Kulon Progo and

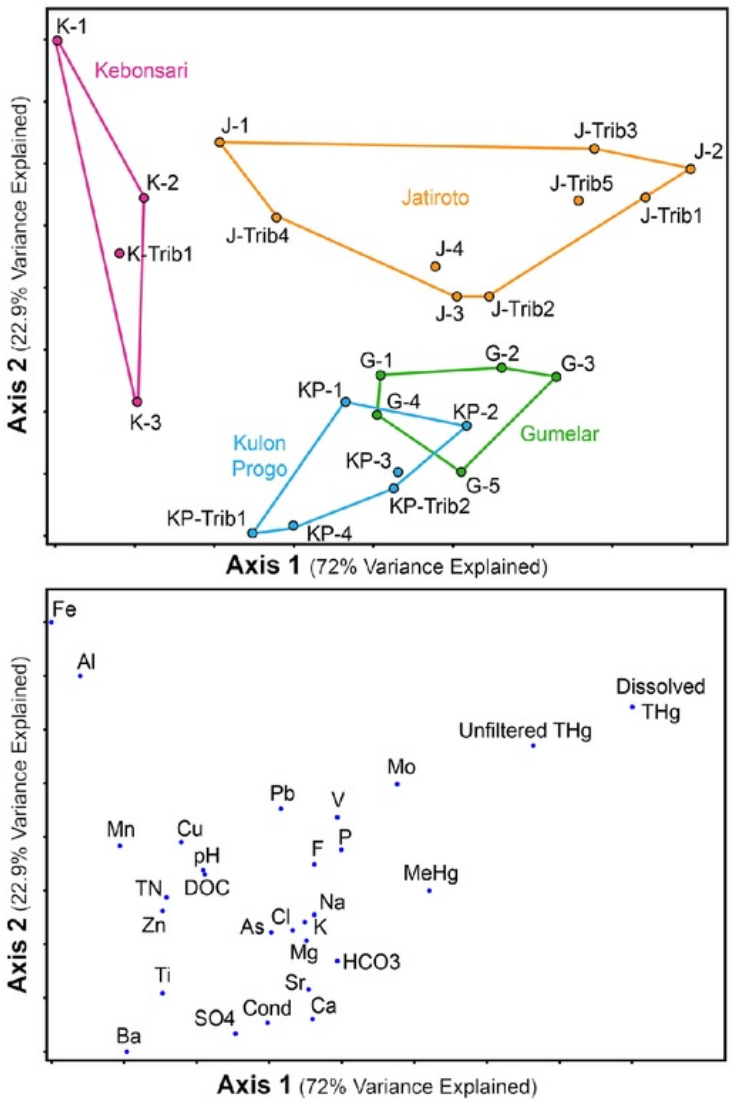

Fig. 4 NMS ordination plot showing the trace and major element chemistry of river samples collected in the study. Axis 1 explains 72% of the variability in the dataset and axis 2 explains an additional 22.9%. The top panel shows that water samples from the four sites plot separately from each other due to different chemistries. The bottom panel shows the distribution of elements controlling axis 1 and axis 2

Gumelar (Fig. 4). Samples from Kebonsari plotted on the left side of the NMS plot and varied more along axis 2 than axis 1. These samples had the highest Fe, Al, Mn, Cu, and Zn concentrations with the lowest THg concentrations and dissolved ion concentrations. Samples from Jatiroto plotted in three distinct groups: relatively clean upstream samples (J-1, J-Trib4) on the left side, samples adjacent to amalgamator inputs (J-2, J-Trib1, J-Trib3, J-Trib5) on the right side, and samples downstream of amalgamator inputs (J-3, J-4, J-Trib2) in the middle. Most of the variation in the Jatiroto samples was due to high THg concentrations in samples adjacent to amalgamator inputs and low THg concentrations upstream of mining activities. Samples from Kulon Progo and Gumelar plotted in overlapping NMS space, with moderate THg concentrations and similar trace and major element chemistry.

3.3 Total and Methyl Mercury Comparison Across Sites

Particulate (> 0.45 μm) and dissolved (< 0.45 μm) THg concentrations varied by orders of magnitude across sites, ranging from 0.42 to 4673 ng/L and 0.81 to 57 ng/L, respectively (Fig. 5 and Table 1). Most THg was found in

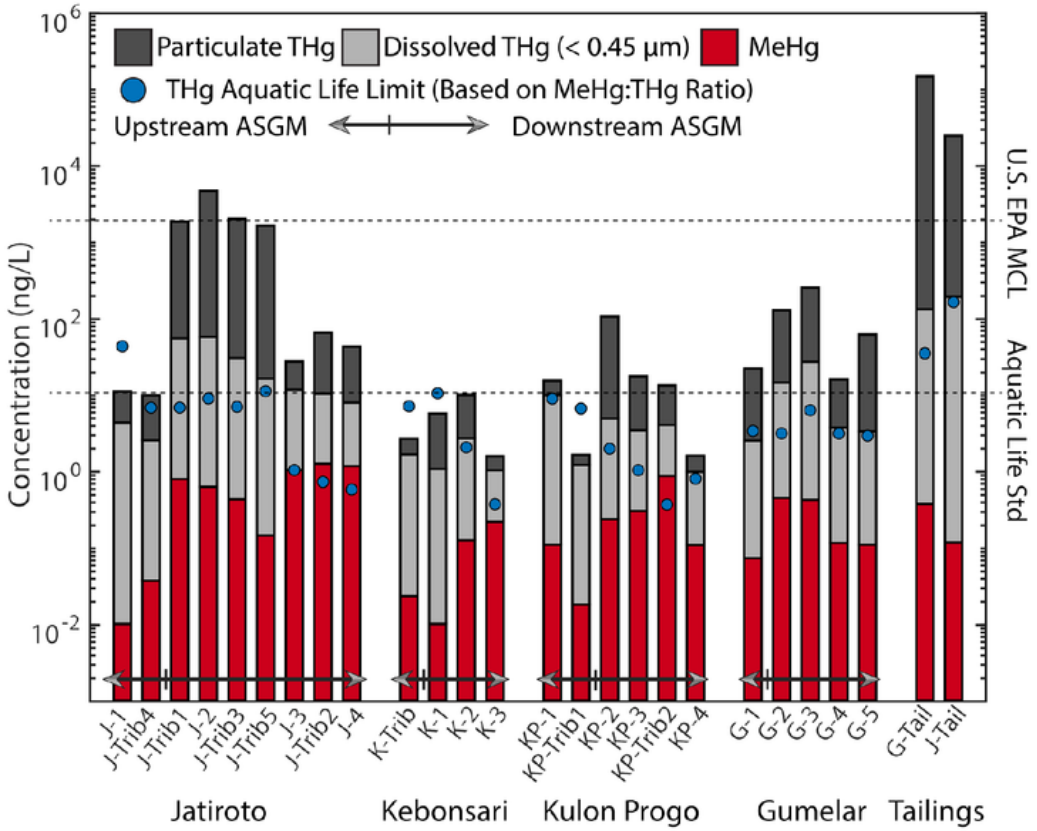

Fig. 5 Dissolved (< 0.45 µm) and particulate (> 0.45 µm) THg concentrations and dissolved MeHg concentrations in water samples collected from Jatiroto, Kebonsari, Kulon Progo, and Gumelar. Samples are ordered from high to low elevation within each ASGM area. Dashed lines correspond to Hg standards: USEPA Maximum Contaminant Level (MCL) standard for aquatic life. Blue dots indicate samples that exceed the British Columbia THg aquatic life limit based on the filtered MeHg to filtered THg ratio. Note logarithmic scale

the particulate fraction, ranging from 75 to 99% near ASGM tailing inputs to as low as 40% at downstream sites. Dissolved THg concentrations exceeded the USEPA aquatic life standard (12 ng/L) in 6 out of 24 river samples but did not exceed the USEPA drinking water maximum contaminant limit (MCL) (2000 ng/L). Dissolved and particulate THg concentrations were highest downstream of mining operations in Jatiroto (2.51–57.0 ng/L and 6.74–4673 ng/L, respectively). Dissolved and particulate THg concentrations in Gumelar were the second highest (2.46–27.0 ng/L and 12.3–228 ng/L, respectively), while concentrations at Kulon Progo were third highest (0.87–9.90 ng/L and 0.42–101 ng/L, respectively). The lowest dissolved and particulate THg concentrations were found in Kebonsari (0.81–2.58 ng/L and 1.35–9.89 ng/L, respectively). Baseline THg concentrations upstream of ASGM activities were slightly higher than worldwide background levels (Nriagu 1990) but comparable to baselines in Ecuadorian ASGM areas (Carling et al. 2013) (Table 2). Unfiltered THg concentrations in the two tailings samples were orders of magnitude higher than concentrations in river samples with values of 24,800 and 150,000 ng/L. The highest THg concentrations were generally found in locations with the highest turbidity (Fig. 6).

MeHg concentrations ranged from < 0.02 to 1.26 ng/L (Fig. 5). MeHg concentrations were higher downstream of ASGM processing sites relative to upstream in Jatiroto, Kulon Progo, and Gumelar. Based on guidelines from British Columbia, Canada, dissolved MeHg:THg concentrations exceeded aquatic life criteria in 17 out of 24 samples (Fig. 5). MeHg:THg ratios ranged from <0.1% to 27% across the study area, with the highest ratios occurring downstream of ASGM processing locations (Fig. 7).

Table 2 THg and MeHg concentrations relative to other studies

Locations	THg particulate (>0.45 μm) (ng/L)	THg dissolved (<0.45 μm) (ng/L)	MeHg dissolved (<0.45 μm) (ng/L)
ASGM sites, Java, Indonesia (this study)			
ASGM tailings	24,600–150,000	133–194	0.12–0.38
Streams below ASGM activities	0.54–4670	0.81–57.0	0.07–1.26
"Uncontaminated" baselines	0.42–19.7	1.1–9.9	0.01–0.11
Comparative values			
Indonesian streams affected by mining[a*]	6.0–9070	–	–
Amazon upstream from mining[b]	1.1–11.6	0.2–7.0	0.00–0.01
Amazon downstream of mining[b]	6.3–84,776	1.2–617.0	0.0–1.1
Antarctica streams and lakes[c*]	0.27–1.9	–	0.02–0.33
Worldwide background rivers and lakes[d*]	0.1–3.5	–	–

[a] Sari et al. (2016); Tomiyasu et al. (2013); Yasuda et al. (2011)

[b] Carling et al. (2013); Gray et al. (2002)

[c] Lyons et al. (1999)

[d] Nriagu (1990)

*These values reflect unfiltered THg concentrations because the study did not distinguish between particulate and dissolved THg

4 Discussion

4.1 Mercury Concentrations in Rivers Not Proportional to Scale of Mining

THg concentrations were not proportional to the scale of mining across the four ASGM areas. The primary gold processing method at each site was whole-ore amalgamation, the most inefficient ASGM practice where an estimated 45–75% of Hg is lost to the aquatic environment (AMAP/UNEP 2013). Assuming miners use 1 kg Hg per amalgamator barrel per day, the flux to the aquatic environment can be estimated from the number of amalgamator barrels. This results in an estimated Hg flux of 4.9–7.7 t/year at Kulon Progo, the site with the fewest amalgamators, and 493–767 t/year at Gumelar, the site with the most amalgamators (Table 1). Jatiroto had the highest THg concentrations in the river but was only the third largest mining area (100 amalgamator barrels). Gumelar was the largest mining area but only had the second highest THg concentrations in the river downstream of ASGM activities.

Several factors may explain the difference between THg concentrations and the estimated Hg flux including watershed characteristics that dilute or limit Hg transport from amalgamator tailings to downstream locations (Hurley et al. 1995). The differences in concentrations may be related to river discharge and relative amount of dilution across watersheds. Using watershed area as a proxy for discharge, Kebonsari had the highest discharge and the lowest THg concentrations. Likewise, Jatiroto had the smallest discharge and the highest THg concentrations. However, the differences in discharge were not large enough to account for the 400-fold differences in THg concentration across sites. Further work is needed to compare THg loads in each watershed relative to the estimated Hg flux from ASGM activities.

The proximity of ASGM processing sites to rivers likely affects Hg transport in each area. Since most Hg contamination from ASGM sites is in the particulate form, ASGM tailings located near riverbanks are transported more easily than tailings located further from the river. For example, ASGM processing activities in Kebonsari occur on a hill located several hundred meters from the river. While Hg use was ten times that of Kulon Progo and three times that of Jatiroto, THg concentrations in Kebonsari were probably lower because of the distance between tailings and the river (Fig. 6). Likewise, many ASGM processing sites in Gumelar were located on a hill away from the river. While some amalgamator waste discharged directly to the river, other waste spilled down the hill and soaked into the soil or tailings pits before reaching the river. In contrast, ASGM processing sites in Kulon Progo and Jatiroto

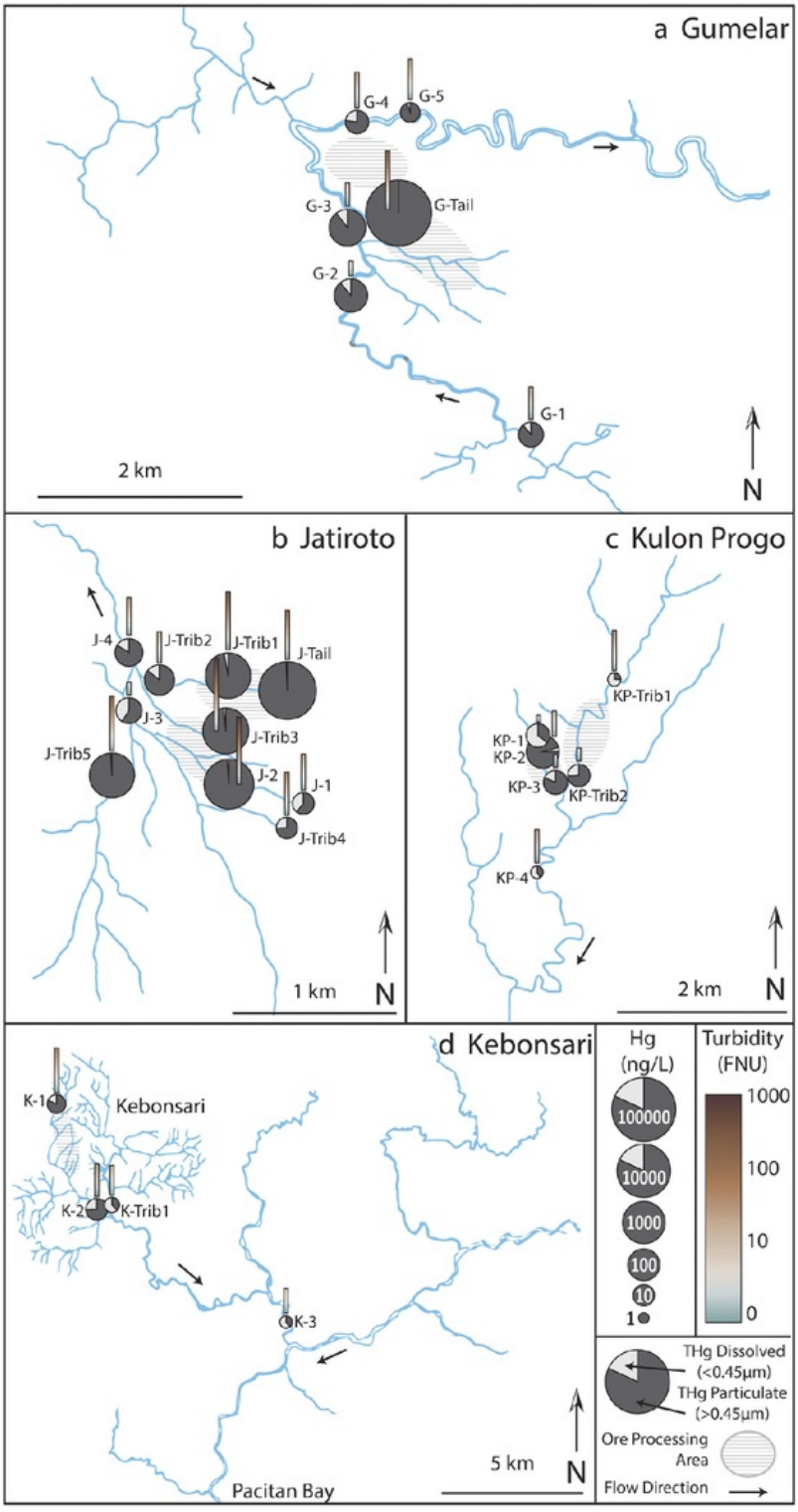

Fig. 6 Turbidity and dissolved (< 0.45 µm) and particulate (> 0.45 µm) THg concentrations in water samples from ASGM areas. **a** Gumelar. **b** Jatiroto. **c** Kulon Progo. **d** Kebonsari

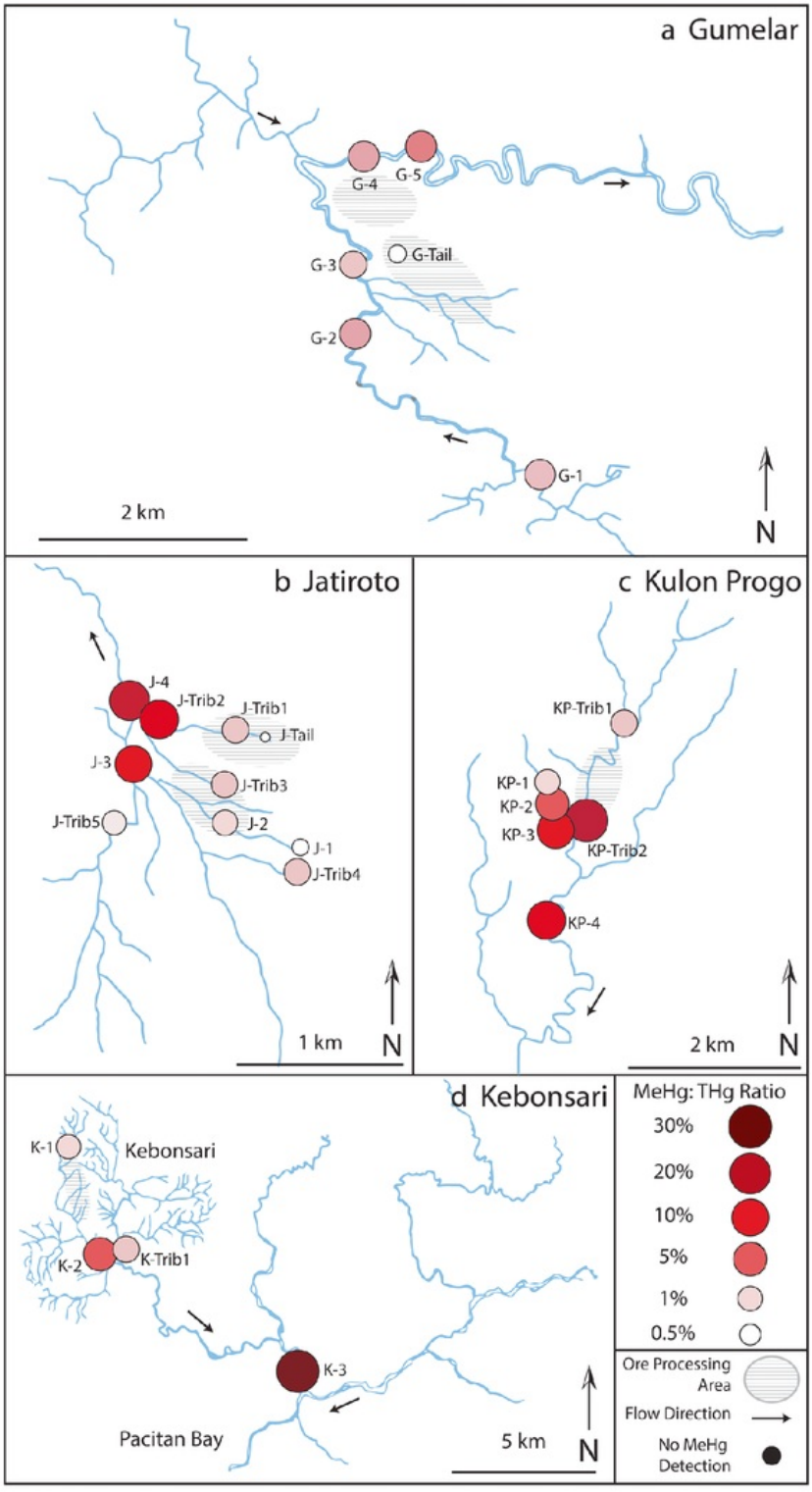

Fig. 7 Ratio of filtered MeHg to filtered THg (< 0.45 μm) in water samples from ASGM areas. **a** Gumelar. **b** Jatiroto. **c** Kulon Progo. **d** Kebonsari

were located directly on the riverbank or discharged directly into nearby streams, increasing availability for aquatic transport.

4.2 Decreasing Hg Concentrations Downstream of Mining Areas

THg concentrations in river water decreased over short distances (< 1 km) downstream of ASGM processing locations (Fig. 6). Many factors may enhance or hinder Hg transport including dilution from incoming streams or groundwater, low stream flow during the dry season, and the chemical behavior of Hg in high pH, $Ca(HCO_3)_2$ waters.

Decreasing THg concentrations are likely a result of stream dilution. For example, dissolved THg decreased 87% after a large tributary joined the ASGM-impacted river between sites G-3 and G-4 in Gumelar (Fig. 6). Dilution was also important in Kebonsari where stream size increased with the addition of multiple non-ASGM affected tributaries between K-2 and K-4. Dissolved THg concentrations at K-2 were 57% higher than the unaffected tributary stream (K-Trib1). Downstream, after the addition of several major tributaries, dissolved THg concentrations at K-3 were the lowest measured in the entire study at 0.81 ng/L. At Kulon Progo, dissolved THg concentrations decreased by almost an order of magnitude after the addition of a large tributary between KP-3 and KP-4 (Fig. 6).

Dilution by groundwater likely contributes to decreasing THg concentrations at Jatiroto, where there are no major tributaries between the sampling sites. Although Jatiroto was the smallest study area, δD and $\delta^{18}O$ values varied the most and were much less depleted downstream (J-3, J-4, J-Trib2) relative to upstream sites, suggesting inputs from groundwater along the river reach (Supplementary material, Fig. S1). Over the same distance, dissolved THg decreased one order of magnitude without the addition of major tributaries (Fig. 6). In contrast, δD and $\delta^{18}O$ changed very little downstream of ASGM operations at the other sites suggesting minimal inputs from groundwater.

Particulate THg concentrations decreased downstream of mining areas likely due to settling. The majority of Hg in ASGM tailings (> 99%) and river water adjacent to ASGM tailings (75–99%) is transported as particulate THg (> 0.45 μm) (Fig. 6). During low flows in the dry season, particulate Hg attached to suspended particles may settle to the river bottom (Limbong et al. 2003). Decreasing water turbidity along the river downstream of ASGM areas show that suspended sediment settled rapidly (Fig. 6). For example, turbidity decreased up to two orders of magnitude just 1 km downstream of ASGM inputs at Jatiroto between sites J-2 and J-3. Over the same distance, particulate THg concentrations also decreased by two orders of magnitude. The turbidity likely decreased along this river reach as water is diverted to irrigate terraced rice fields, allowing particles to settle in the agricultural areas. Similarly, at Kebonsari, water is diverted to irrigate rice fields between sites K-1 and K-2. The stagnant fields combined with low stream flow likely promote settling and hinder particulate Hg transport.

High stream flow in the wet season may remobilize particulate Hg from the streambed, erode contaminated soils from the riverbanks in ASGM areas, and transport Hg from tailings piles via overland flow. During the wet season (November through March), monthly precipitation in Central Java increases up to 10 times over that of the dry season. Since Hg transport from mining areas is highly episodic and occurs during intense precipitation and runoff events (Whyte and Kirchner 2000; Pattelli et al. 2014), Hg concentrations are likely higher in the rainy season. Floodwaters may transport Hg and other heavy metals from contaminated mining areas into rice fields where it can be methylated and bioaccumulate in crops and fish. Further study is needed to investigate Hg transport in the wet season when rainfall and high stream discharge may mobilize contaminated sediment near mining areas.

THg concentrations are also impacted by water chemistry. Hg may be transported as a dissolved ion, as a complex with dissolved organic matter, or adsorbed to finely suspended particles like clay depending on major ion chemistry, pH, and temperature (Gaillardet et al. 2003; Fitzgerald and Lamborg 2003). Except for the tailings samples and the sample from site K-1, all samples had a pH greater than 7, favoring Hg-mineral precipitation and sorption. Saturation indices (SIs) indicated that the Hg-containing mineral montroydite (HgO) was oversaturated for all river samples but K-1 (Supplementary material, Table S4). Tiemannite (HgSe) was also oversaturated in every sample that contained trace amounts of selenium. Dissolved THg in stream samples is likely bound to small organic colloidal particles (> 0.2 to < 0.45 μm) (Babiarz et al. 2001). However, we found no relationship between DOC and THg

concentrations, which is common in mining areas where large amounts of inorganic Hg are added to streams (Shanley and Bishop 2012).

4.3 Increased Fraction of Methyl Mercury Downstream of Mining Areas

MeHg concentrations were highest downstream of ASGM areas at Jatiroto, Kulon Progo, and Gumelar (Fig. 5). While concentrations provide useful information, MeHg:THg ratios are often used to understand in situ methylation processes (Mitchell et al. 2008). Dissolved MeHg:THg ratios varied by orders of magnitude across study sites from 0.02 to over 27%, indicating different rates of in situ MeHg production (Fig. 7). The normal background MeHg:THg ratio in freshwater is approximately 1% (Gray and Hines 2009). Ratios > 10% at J-3, J-4, J-Trib2, K-3, KP-3, and KP-4 KP-Trib1 indicate substantial methylation occurred at these sites.

Even small ASGM areas like Kulon Progo (30 amalgamator barrels) had MeHg:THg ratios above recommended aquatic life limits (Fig. 5). Furthermore, other studies that measured similar aquatic Hg concentrations found elevated Hg levels in fish downstream of ASGM areas (Limbong et al. 2003; Castilhos et al. 2006; Tomiyasu et al. 2013). Rice cultivated with ASGM tailings water on Lombok also contained elevated MeHg levels (Krisnayanti et al. 2012). The rice is typically sold across Indonesia and consumption is not limited to the small ASGM community.

Methylation occurs in anoxic environments such as wetlands and rice fields where SO_4 and dissolved organic materials are available (Todorova et al. 2009). While none of the river samples were anoxic, they were all taken near sites with extensive agricultural runoff from rice paddies. Rice fields promote Hg methylation and bioaccumulation because they alternate between wet and dry conditions, which creates anoxia (Kirk 2004; Rothenberg et al. 2014). Rice roots also supply a wide variety of DOC compounds which enhance Hg-methylation (Rothenberg et al. 2014). MeHg concentrations in rice are up to 40 times higher than other crops cultivated in similar soil (Qiu et al. 2008). Therefore, rice fields cultivated downstream of ASGM processing areas with Hg-laden water likely produce and bioaccumulate MeHg. Further research is needed to quantify Hg methylation processes in rice and fish cultivation areas that are located downstream of ASGM areas.

4.4 Comparison to Other Studies and Global Averages

THg concentrations upstream, within, and downstream of ASGM areas in our study area were comparable to other ASGM areas in Indonesia and worldwide. Baseline THg concentrations upstream of ASGM activities were elevated compared to the worldwide non-mining background in rivers and lakes (Nriagu 1990) but similar to other ASGM areas (Table 2). For example, background THg values across tropical ASGM processing sites in Ecuador ranged between 1.1 and 11.6 ng/L (Carling et al. 2013), the same range as baselines measured in this study. Baseline values at our background sites are likely elevated in comparison to worldwide (nonmining) background because of the widespread use of elemental Hg and redeposition of Hg vapor in the region or additional (unknown) ASGM activities upstream of the sampling sites.

The spatial variability in THg concentrations we observed downstream of ASGM activities is consistent with other studies in Indonesia. For example, THg concentrations in seven samples spaced every 50 m from upstream to downstream of ASGM activities in Gumelar varied by orders of magnitude with an average downstream THg concentration of 270 ng/L (Sari et al. 2016). These concentrations were an order of magnitude higher than those we measured along the same stretch (G-4, G-5), suggesting that THg concentrations fluctuate depending on the conditions during sampling even in the same area. Another study of an ASGM area in North Sulawesi found that THg concentrations in river water changed by orders of magnitude from upstream to downstream of mining areas *and* across three sampling trips spaced 2 weeks apart in May–June (Limbong et al. 2003). The authors concluded that particulate Hg rapidly attached to suspended sediment and settled to the river bottom. THg concentrations measured along the Cikaniki River, which runs through an ASGM near Jakarta in West Java, also varied from 90 to 9070 ng/L in one study and 120–440 ng/L in another (Tomiyasu et al. 2013; Yasuda et al. 2011). A third study in Bombana, Southeast Sulawesi, found that THg concentrations increased by six orders of magnitude from upstream to downstream of ASGM processing sites during the dry season (Beavis and McWilliam 2018).

5 Conclusions

ASGM activities in Central Java, Indonesia, contributed a substantial amount of Hg pollution to local streams. THg concentrations increased by orders of magnitude downstream of ASGM areas relative to upstream or unaffected stream samples. The majority of Hg from ASGM activities was in the particulate (> 0.45 μm) fraction. During low-flow conditions in the dry season, THg concentrations decreased by orders of magnitude over short distances from ASGM processing sites (< 1 km) as particulate Hg likely settles to the streambed. In the wet season, high flows may remobilize contaminated sediment from the streambed and erode Hg-laden tailings piles. Therefore, our results likely represent a conservative estimate of Hg contamination and THg concentrations are potentially higher downstream of mining areas during the wet season.

The scale of mining at each area (estimated by the number of amalgamator barrels) was not proportional to THg concentrations in affected streams, indicating that even small mining areas may negatively impact water quality. Hg concentrations were relatively higher in rivers with ASGM processing sites located near the riverbank (Kulon Progo, Jatiroto) and lower at sites with processing activity located farther from the river (Gumelar, Kebonsari). The dissolved MeHg:THg ratio, an indicator of in situ methylation processes, ranged from < 0.1 to 27% downstream of ASGM processing areas. High ratios (> 10%) were measured in samples near agricultural and rice paddy runoff, indicating that these areas have a high potential for MeHg production. In each of the study areas, Hg-laden streams are diverted to irrigate rice fields where inorganic Hg can be converted to toxic MeHg. Further study is needed to determine Hg bioaccumulation rates in rice, fish, and other crops cultivated downstream of these ASGM areas.

Acknowledgments Research permits were obtained through Kemenristekdikti, the Indonesian foreign research permitting office (Govt. Regulation no. 41/2006). We are thankful for students and faculty at the Geological Engineering Department of Universitas Pembangunan Nasional (UPN) "Veteran" in Yogyakarta for their assistance and support in conducting this research. We also thank regional and local Indonesian government agencies and leaders that assisted in this research including: the Department of Energy and Natural Resources Central Java Province (Dinas Energi dan Sumber Daya Mineral Provinsi Jawa Tengah), the Department of Mining and Energy in Pacitan East Java Province (Dinas Pertambangan dan Energi Kabupaten Pacitan Jawa Timur), Bpk. Harsono and Bpk. Ketik, and the gracious village leaders who welcomed us into their homes and helped us conduct this research.

Funding Information Funding was provided by a Geological Society of America Graduate Student Research Grant and a Foreign Language Area Studies (FLAS) fellowship from the US Department of Education through Brigham Young University.

References

AMAP/UNEP (2013). AMAP/UNEP technical background report for the global mercury assessment 2013: final technical report; output.

Babiarz, C. L., Hurley, J. P., Hoffmann, S. R., Andren, A. W., Shafer, M. M., & Armstrong, D. E. (2001). Partitioning of total mercury and methylmercury to the colloidal phase in freshwaters. *Environmental Science & Technology, 35*(24), 4773–4782.

Beavis, S., McWilliam, A. (2018). Muddy rivers and toxic flows: Risks and impacts of artisanal gold-mining in the riverine catchments of Bombana, Southeast Sulawesi (Indonesia). Between the Plough and the Pick: Informal, Artisanal and Small-scale Mining in the Contemporary World, 295–310.

Bethke, C., Farrell, B., Yeakel, S. (2018). The Geochemist's workbench, version 12.0: GWB essentials guide. Aqueous solutions, LLC, Champaign, Illinois, US.

Bishop, K., Lee, Y.-H., Pettersson, C., & Allard, B. (1995). Methylmercury in runoff from the Svartberget catchment in northern Sweden during a stormflow episode. In *Mercury as a Global Pollutant* (pp. 221-224): Springer.

Bose-O'Reilly, S., Drasch, G., Beinhoff, C., Rodrigues-Filho, S., Roider, G., Lettmeier, B., et al. (2010). Health assessment of artisanal gold miners in Indonesia. *Science of the Total Environment, 408*(4), 713–725.

Carling, G. T., Diaz, X., Ponce, M., Perez, L., Nasimba, L., Pazmino, E., et al. (2013). Particulate and dissolved trace element concentrations in three southern Ecuador rivers impacted by artisanal gold mining. *Water, Air, & Soil Pollution, 224*(2), 1415.

Castilhos, Z. C., Rodrigues-Filho, S., Rodrigues, A. P. C., Villas-Bôas, R. C., Siegel, S., Veiga, M. M., et al. (2006). Mercury contamination in fish from gold mining areas in Indonesia and human health risk assessment. *Science of the Total Environment, 368*(1), 320–325.

Clarkson, T. W. (1997). The toxicology of mercury. *Critical Reviews in Clinical Laboratory Sciences, 34*(4), 369–403.

Elvince, R., Inoue, T., Tsushima, K., Takayanagi, R., Darung, U., Gumiri, S., et al. (2008). Assessment of mercury contamination in the Kahayan river, Central Kalimantan, Indonesia. *Journal of Water and Environment Technology, 6*(2), 103–112.

Fitzgerald, W., & Lamborg, C. (2003). Geochemistry of mercury in the environment. *Treatise on geochemistry, 9*, 612.

Gaillardet, J., Viers, J., & Dupré, B. (2003). Trace elements in river waters. *Treatise on geochemistry, 5*, 605.

Gray, J. E., Labson, V. F., Weaver, J. N., & Krabbenhoft, D. P. (2002). Mercury and methylmercury contamination related to artisanal gold mining, Suriname. *Geophysical Research Letters, 29*, 2105.

Gray, J. E., & Hines, M. E. (2009). Biogeochemical mercury methylation influenced by reservoir eutrophication, Salmon Falls Creek Reservoir, Idaho, USA. *Chemical Geology, 258*(3–4), 157–167.

Harijoko, A., Htun, T. M., Saputra, R., Warmada, I. W., Setijadji, L. D., Imai, A., et al. (2010). Mercury and arsenic contamination from small scale gold mining activities at Selogiri area, Central Java, Indonesia. *Journal of Applied Geology, 2*(1).

Hurley, J. P., Benoit, J. M., Babiarz, C. L., Shafer, M. M., Andren, A. W., Sullivan, J. R., et al. (1995). Influences of watershed characteristics on mercury levels in Wisconsin rivers. *Environmental Science & Technology, 29*(7), 1867–1875. https://doi.org/10.1021/es00007a026.

Hurley, J. P., Cowell, S. E., Shafer, M. M., & Hughes, P. E. (1998). Tributary loading of mercury to Lake Michigan: Importance of seasonal events and phase partitioning. *Science of the Total Environment, 213*(1–3), 129–137.

IAEA/WMO. (2019). *Global network of isotopes in precipitation*. The GNIP Database. Accessible at: https://nucleus.iaea.org/wiser.

Iqbal, R., & Inoue, T. (2011). Mercury pollution in Java Island: Past and present. *Journal of Ecotechnology Research, 16*(2), 51–57.

Ismawati, Y., Petrlik, J., Digangi, J. (2013). *Mercury hotspots in Indonesia*.

Kirk, G. (2004). *The biogeochemistry of submerged soils*. John Wiley & Sons.

Krisnayanti, B. D., Anderson, C. W., Utomo, W. H., Feng, X., Handayanto, E., Mudarisna, N., et al. (2012). Assessment of environmental mercury discharge at a four-year-old artisanal gold mining area on Lombok Island, Indonesia. *Journal of Environmental Monitoring, 14*(10), 2598–2607.

Limbong, D., Kumampung, J., Rimper, J., Arai, T., & Miyazaki, N. (2003). Emissions and environmental implications of mercury from artisanal gold mining in north Sulawesi, Indonesia. *Science of the Total Environment, 302*(1–3), 227–236.

Luoma, S. N. (1983). Bioavailability of trace metals to aquatic organisms—A review. *Science of the Total Environment, 28*(1–3), 1–22.

Lyons, W. B., Welch, K. A., & Bonzongo, J. C. (1999). Mercury in aquatic systems in Antarctica. *Geophysical Research Letters, 26*, 2235–2238.

Mansfield, C. R., & Black, F. J. (2015). Quantification of monomethylmercury in natural waters by direct ethylation: Interference characterization and method optimization. *Limnology and Oceanography: Methods, 13*(2), 81–91.

McCune, B., Mefford, M. (1999). PC-ORD: multivariate analysis of ecological data; Version 4 for Windows;[User's Guide]: MjM software design.

Mitchell, C. P., Branfireun, B. A., & Kolka, R. K. (2008). Spatial characteristics of net methylmercury production hot spots in peatlands. *Environmental Science & Technology, 42*(4), 1010–1016.

Nakazawa, K., Nagafuchi, O., Kawakami, T., Inoue, T., Yokota, K., Serikawa, Y., et al. (2016). Human health risk assessment of mercury vapor around artisanal small-scale gold mining area, Palu city, Central Sulawesi, Indonesia. *Ecotoxicology and Environmental Safety, 124*, 155–162.

NRC (2000). Toxicological effects of methylmercury: National Academies Press.

Nriagu, J. O. (1990). Human influence on the global cycling of trace metals. *Palaeogeography, Palaeoclimatology, Palaeoecology, 82*(1–2), 113–120.

Obrist, D., Kirk, J. L., Zhang, L., Sunderland, E. M., Jiskra, M., & Selin, N. E. (2018). A review of global environmental mercury processes in response to human and natural perturbations: Changes of emissions, climate, and land use. *Ambio, 47*(2), 116–140.

Pattelli, G., Rimondi, V., Benvenuti, M., Chiarantini, L., Colica, A., Costagliola, P., et al. (2014). Effects of the November 2012 flood event on the mobilization of Hg from the Mount Amiata Mining District to the sediments of the Paglia River Basin. *Minerals, 4*(2), 241–256.

Qiu, G., Feng, X., Li, P., Wang, S., Li, G., Shang, L., et al. (2008). Methylmercury accumulation in rice (Oryza sativa L.) grown at abandoned mercury mines in Guizhou, China. *Journal of Agricultural and Food Chemistry, 56*(7), 2465–2468.

Rothenberg, S. E., Windham-Myers, L., & Creswell, J. E. (2014). Rice methylmercury exposure and mitigation: A comprehensive review. *Environmental Research, 133*, 407–423.

Rothenberg, S. E., Yin, R., Hurley, J. P., Krabbenhoft, D. P., Ismawati, Y., Hong, C., et al. (2017). Stable mercury isotopes in polished rice (Oryza Sativa L.) and hair from rice consumers. *Environmental Science & Technology, 51*(11), 6480–6488.

Sari, M. M., Inoue, T., Matsumoto, Y., & Yokota, K. (2016). Measuring total mercury due to small-scale gold mining activities to determine community vulnerability in Cihonje, Central Java, Indonesia. *Water Science and Technology, 73*(2), 437–444.

Scheuhammer, A. (1987). The chronic toxicity of aluminium, cadmium, mercury, and lead in birds: A review. *Environmental Pollution, 46*(4), 263–295.

Schuster, P., Shanley, J., Marvin-Dipasquale, M., Reddy, M., Aiken, G., Roth, D., et al. (2008). Mercury and organic carbon dynamics during runoff episodes from a northeastern USA watershed. *Water, Air, and Soil Pollution, 187*(1–4), 89–108.

Shanley, J. B., Bishop, K. (2012). Mercury cycling in terrestrial watersheds. In M. S. Bank (Ed.), *Mercury in the environment* (1 ed., pp. 119–142, Pattern and Process): University of California Press.

Sherman, L. S., Blum, J. D., Basu, N., Rajaee, M., Evers, D. C., Buck, D. G., et al. (2015). Assessment of mercury exposure among small-scale gold miners using mercury stable isotopes. *Environmental Research, 137*, 226–234.

Sigg, L., Behra, P., Stumm, W. (2001). *Chimie des milieux aquatiques*. Dunod.

Smyth, H. R., Hall, R., & Nichols, G. J. (2008). Cenozoic volcanic arc history of East Java, Indonesia: The stratigraphic record of eruptions on an active continental margin. *Special Papers-Geological Society of America, 436*, 199.

Spiegel, S. J., Agrawal, S., Mikha, D., Vitamerry, K., Le Billon, P., Veiga, M., et al. (2018). Phasing out mercury? Ecological economics and Indonesia's small-scale gold mining sector. *Ecological Economics, 144*, 1–11.

Swartzendruber, P., Jaffe, D. (2012). Sources and transport: A global issue. In M. S. Bank (Ed.), *Mercury in the environment* (1 ed., pp. 3–18, Pattern and Process): University of California Press.

Telmer, K. H., Veiga, M. M. (2009). World emissions of mercury from artisanal and small scale gold mining. In *Mercury fate and transport in the global atmosphere* (pp. 131-172): Springer.

Todorova, S. G., Driscoll, C. T., Jr., Matthews, D. A., Effler, S. W., Hines, M. E., & Henry, E. A. (2009). Evidence for regulation of monomethyl mercury by nitrate in a seasonally stratified, eutrophic lake. *Environmental Science & Technology, 43*(17), 6572–6578.

Tomiyasu, T., Kono, Y., Kodamatani, H., Hidayati, N., & Rahajoe, J. S. (2013). The distribution of mercury around the small-scale gold mining area along the Cikaniki river, Bogor, Indonesia. *Environmental Research, 125*, 12–19.

USEPA. (2002). Method 1631, revision E: Mercury in water by oxidation, purge and trap, and cold vapor atomic fluorescence spectrometry, 38 pp.

Whyte, D. C., & Kirchner, J. W. (2000). Assessing water quality impacts and cleanup effectiveness in streams dominated by episodic mercury discharges. *Science of the Total Environment, 260*(1–3), 1–9.

Yasuda, M., Syawal, M. S., Sikder, M. T., Hosokawa, T., Saito, T., Tanaka, S., et al. (2011). Metal concentrations of river water and sediments in West Java, Indonesia. *Bulletin of Environmental Contamination and Toxicology, 87*(6), 669–673.

Comparison of Mercury Contamination in Four Indonesian Watersheds Affected by Artisanal and Small-Scale Gold Mining of Varying Scale

ORIGINALITY REPORT

14%	10%	12%	%
SIMILARITY INDEX	INTERNET SOURCES	PUBLICATIONS	STUDENT PAPERS

MATCH ALL SOURCES (ONLY SELECTED SOURCE PRINTED)

< 1%

★ Dave Waltham. "Basin formation by volcanic arc loading", Special Paper 436 Formation and Applications of the Sedimentary Record in Arc Collision Zones, 2008

Publication

Exclude quotes	Off	Exclude matches	Off
Exclude bibliography	Off		